

Supporting Information (SI)

Two-fold interpenetrated Mn-based Metal-Organic Frameworks (MOFs) as battery-type electrode materials for charge storage

Kuaibing Wang,^{a,b} Bo Lv,^a Zikai Wang,^{a,c} Hua Wu,^{a,*} Jiangyan Xu,^a Qichun Zhang^{b,*}

^a Department of Chemistry, College of Sciences
Nanjing Agricultural University
Nanjing 210095, Jiangsu, P. R. China
E-mail: wuhua@njau.edu.cn

^b School of Materials Science & Engineering
Nanyang Technological University
Singapore 639678, Singapore
E-mail: qc Zhang@ntu.edu.sg

^c College of Resources and Environmental Sciences
Nanjing Agricultural University
Nanjing 210095, Jiangsu, P. R. China

1. Experimental Section

1.1 Synthesis of [Mn(HTATB)(BIB)(DMF)(H₂O)] (SC-7)

A mixture of MnSO₄·H₂O (0.025 g, 0.15 mmol), BIB (0.036 g, 0.15 mmol), H₃TATB (0.044 g, 0.1 mmol), DMF (6 mL) and water (3 mL) was placed in a Teflon reactor (20 mL) and heated at 100 °C for 72 hours. After the mixture naturally cooled down to room temperature at a rate of 10 °C·h⁻¹, colorless crystals of SC-7 were obtained with a yield of 77%. Anal. Calcd for C₄₁H₃₅MnN₈O₈: C, 59.86; H, 4.29; N, 13.62. Found: C, 59.78; H, 4.35; N, 13.58. FTIR (KBr pellet, cm⁻¹): 3320(w), 1694(s), 1655(s), 1565(s), 1362(s), 1278(s), 1098(m), 1008(m), 924(m), 878(w), 782(s), 693(m), 654(m), 620(w).

1.2 Synthesis of [Mn(HTATB)(TIPA)(H₂O)] (SC-8)

In comparison with SC-7, the reaction conditions kept unchanged except that the N-donor ligand BIB was replaced by TIPA (0.044 g, 0.1 mmol) linker. The colorless crystals of SC-8 were obtained in yield of 85% after 72 hours. Anal. Calcd for C₅₁H₃₆MnN₁₀O₇: C, 64.09; H,

3.80; N, 14.65. Found: C, 64.14; H, 3.75; N, 14.70. FTIR (KBr pellet, cm^{-1}): 3483(w), 3084(w), 1678(s), 1515(s), 1368(s), 1267(s), 1115(w), 1059(s), 1019(s), 963(m), 823(m), 772(s), 732(m), 665(m), 547(w).

1.2 CNTs-supported composites

The synthetic method was modified according to our previous work.^{23c} Detailedly, carbon nanotubes (CNTs, 20mg) was introduced into the ethanol solution (20 mL) containing sodium polystyrene sulfonate (PSS, 1 mL). After 30 mins of sonication and the following 30min of stirring, the well-ground Mn-MOFs crystals (80 mg) were added and vigorously stirred another 4 hours. The corresponding solid products were obtained after several rounds of washing and centrifugation. The as-obtained products were labeled as CNTs/SC-7 and CNTs/SC-8, respectively.

1.3 Fabrication of working electrode

Acetylene black (15 mg) and as-synthesized active material (75 mg) were mixed together through grinding. Then, the mixed products were introduced into an isopropanol system containing PTFE (10 mg) and vigorously stirred until the complex distributed uniformly to form a slurry. Nickel foam (size: 1cm \times 5cm) was prepared as a current collector due to the porosity and large contact area and washed it by ethanol several times. The slurry was loaded on chosen nickel foam (area: 1cm \times 1cm) and pressed it by Manual Rolling Press (MR-100A, MTI Corp). Notably, the loading mass ranged in 2.1–3.6 mg.

1.4 Methods and Measurements

The BIB and TIPA ligands were synthesized according to the procedures reported earlier. Other reagents of analytical grade and solvents employed were commercially available and used as received without further purification. Single-crystal X-ray diffraction data for SC-7

and SC-8 were collected with a Bruker Smart CCD Diffraction at a temperature of 293(2) K, using a ω scan technique with Mo-K α radiation ($\lambda = 0.71073 \text{ \AA}$). FT-IR spectra were recorded from KBr pellets in range 4000-400 cm^{-1} on a Nicolet 380FT-IR spectrometer. X-ray photoelectron spectroscopy (XPS), using nonmonochromatized Al $\text{K}\alpha$ X-ray as excitation source, was performed on an ESCALab MKII X-ray photoelectron spectrometer. X-ray powder diffraction (XRD) data were collected on a Bruker D8 Advance instrument using Cu $\text{K}\alpha$ radiation ($\lambda = 1.54056 \text{ \AA}$) at room temperature. Elemental analyses were carried out with a Carlo Erba 1106 elemental analyzer. Thermogravimetric analyses (TGA) were carried out in air atmosphere on a Beijing Hengjiu HTG-1 instrument with a heating rate of 10 $^{\circ}\text{C min}^{-1}$. The morphologies of the as-synthesized electrode products before and after cycling were obtained by using a JEOL JSM-7500F field-emission scanning electron microscope (FE-SEM). The adsorption-desorption isotherms of nitrogen were measured by using a V-Sorb 2800P adsorption equipment (Gold APP Instrument, Beijing, China). All electrochemical measurements (cyclic voltammetry (CV) and charging-discharging test (CD)) were performed with an electrochemical analyzer system, CHI660E (Chenhua Instrument, Shanghai, China) in a three-electrode cell include a platinum wire counter electrode, a saturated calomel electrode (SCE) reference electrode and a working electrode. The electrolyte is KOH aqueous solution (6.0 M). Electrochemical impedance spectroscopy (EIS) measurements of as-synthesized samples were conducted at open-circuit voltage in the frequency range of 100 kHz to 10 mHz.

2. Structural characterization

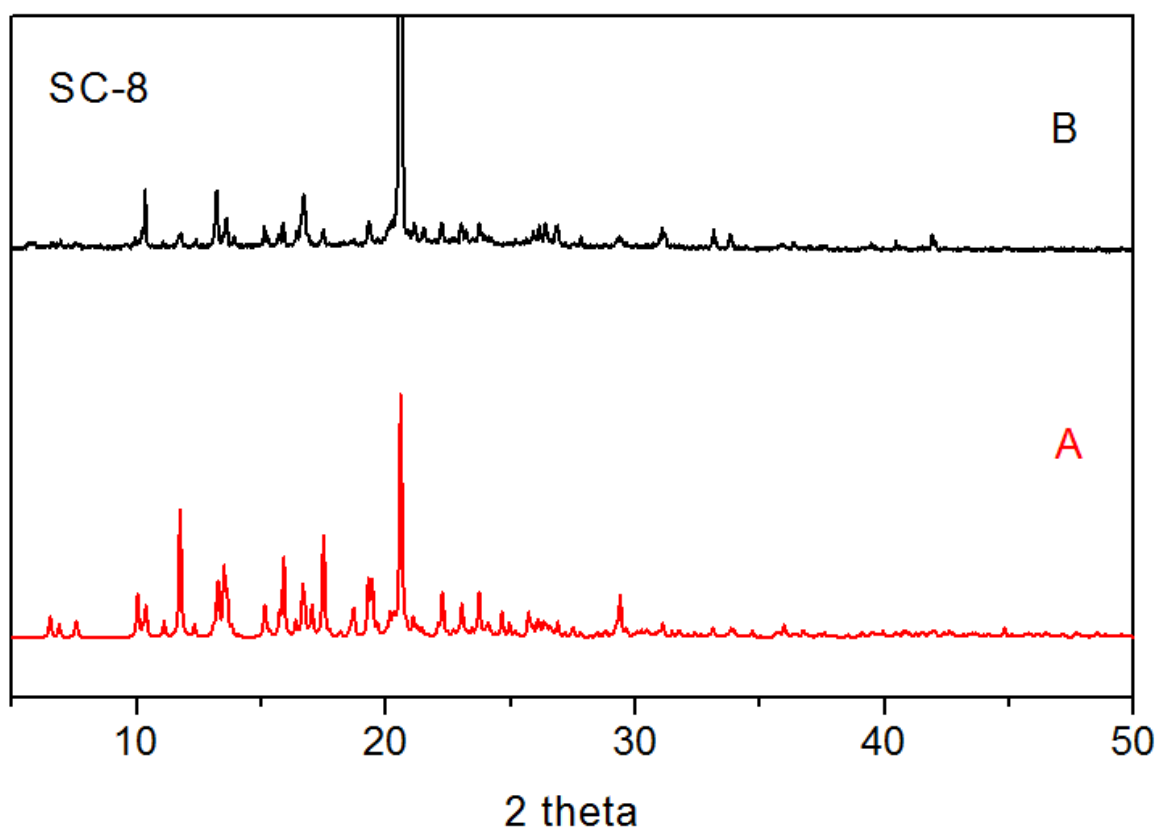
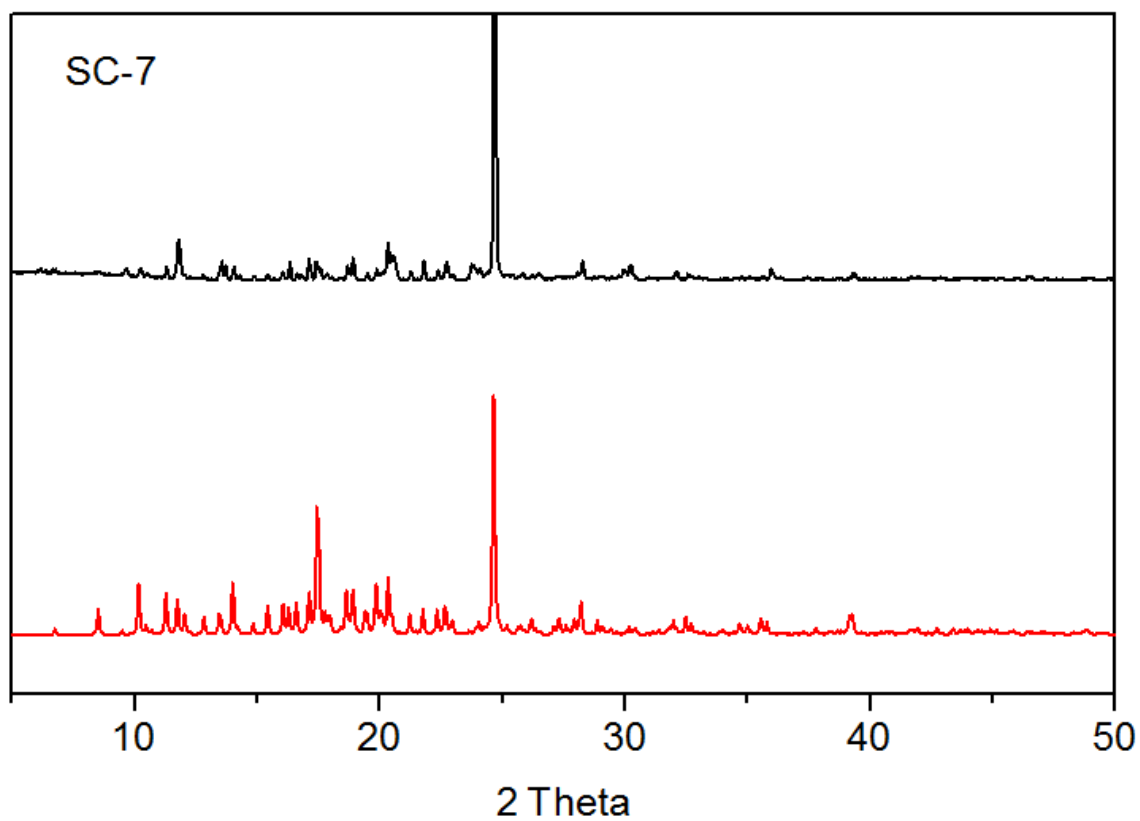


Fig. S1. PXRD patterns of simulated A (red) and measured B (black) PXRD for SC-7 and SC-8.

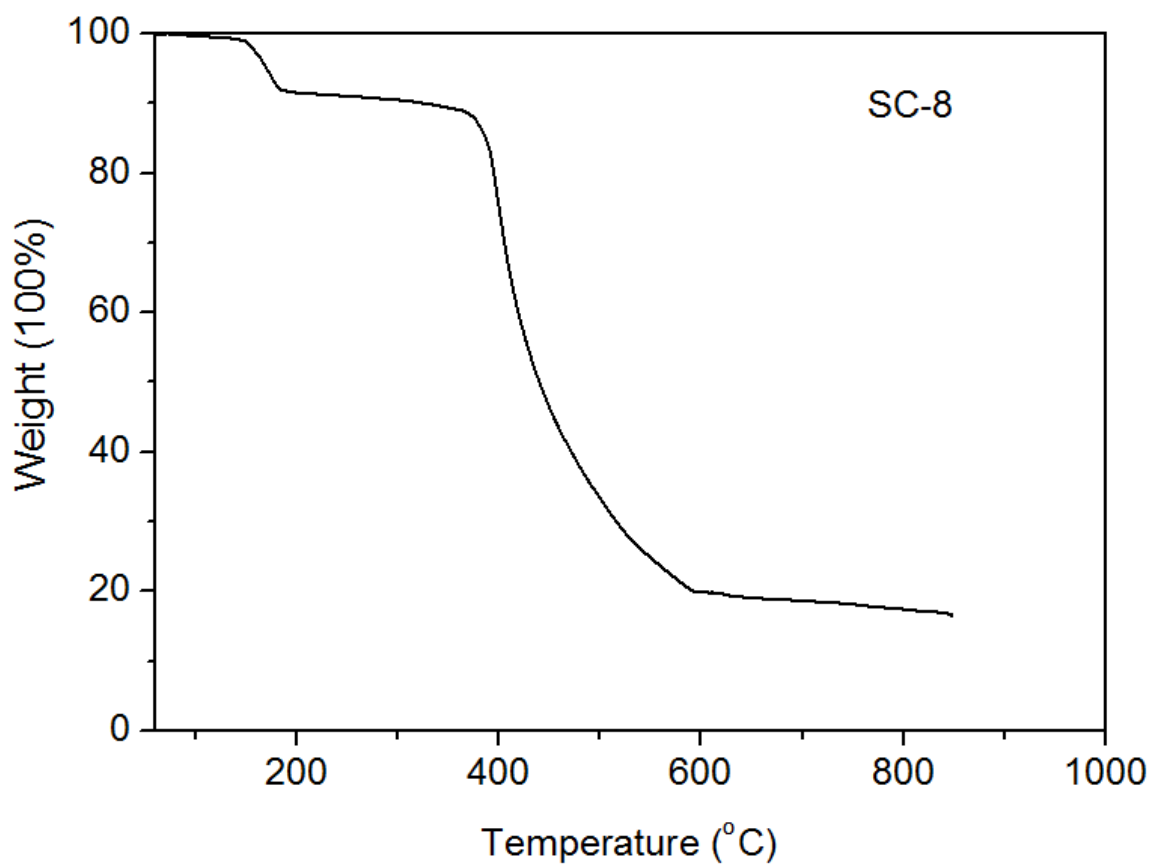
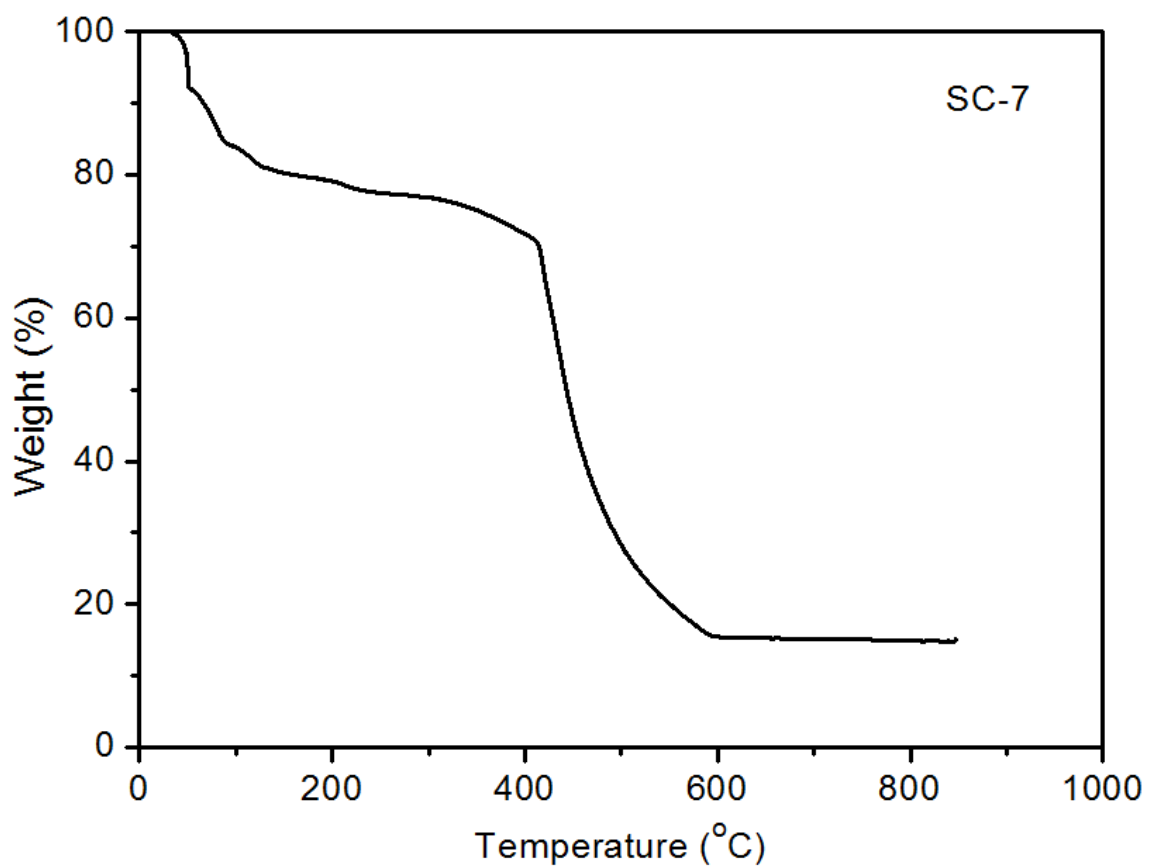


Fig. S2. The TG curves for SC-7 and SC-8.

3. Mechanism analyses

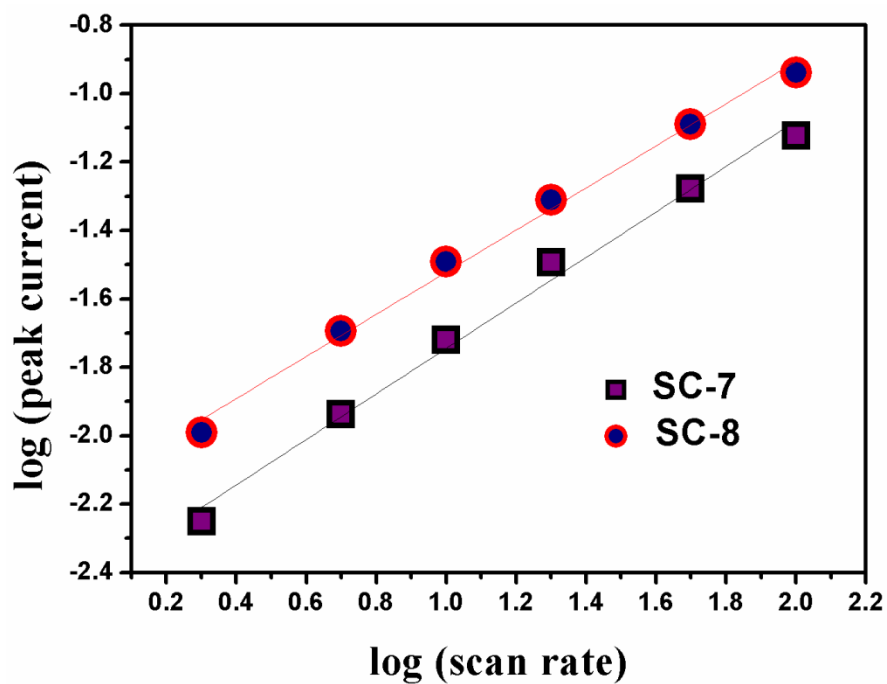


Fig. S3. Power-law dependence of current on sweep rate (using anodic peak value). Square: SC-7 electrode; Circle: SC-8 electrode.

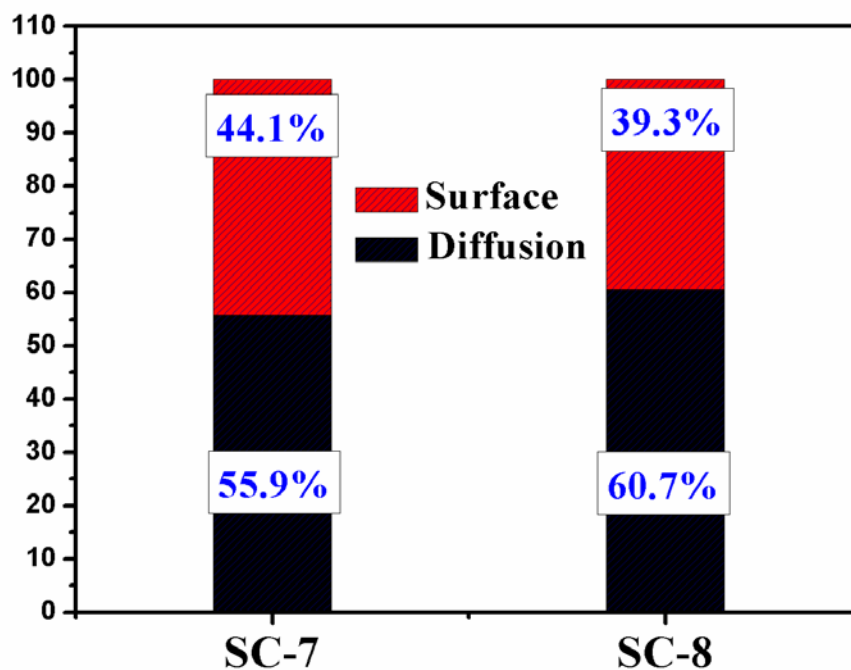


Fig. S4. The histogram of the current contribution ratio (surface- or diffusion-controlled) for SC-7 and SC-8 electrode.

4. Surface characterization

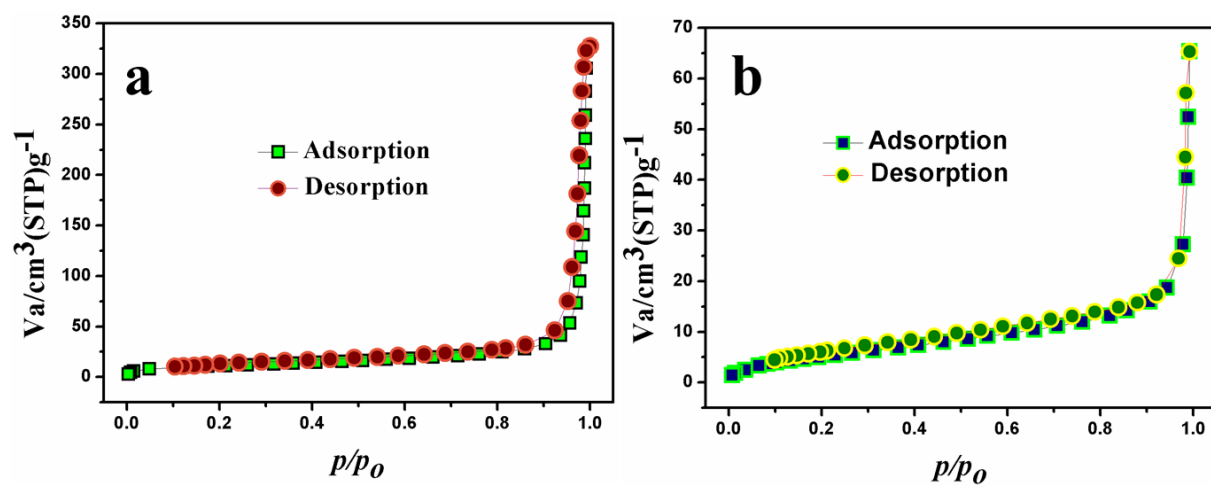


Fig. S5. N_2 adsorption-desorption curves for SC-7 (a) and SC-8 (b), respectively.

5. Electrochemical impedance spectroscopy (EIS) tests

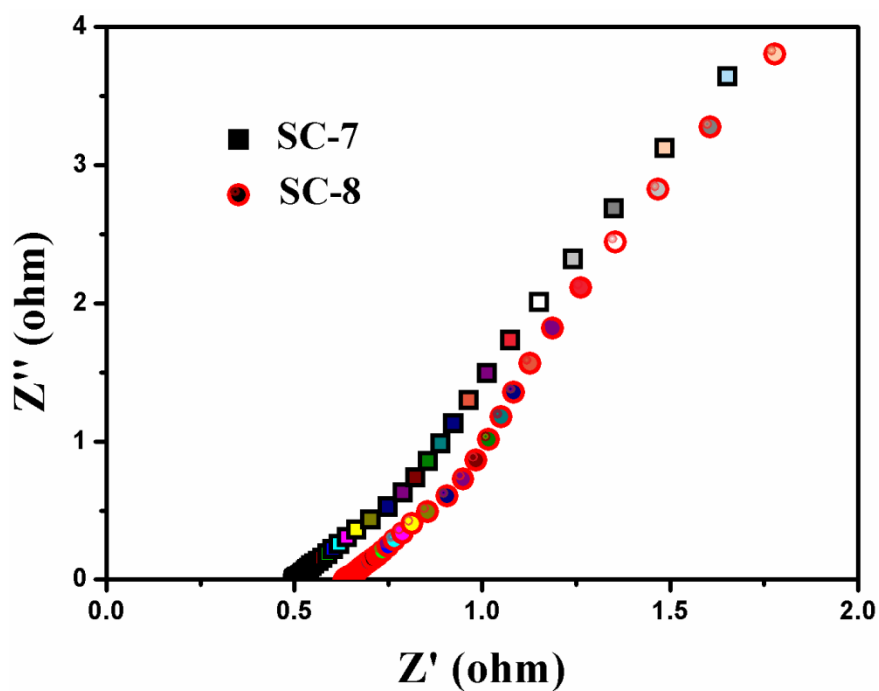


Fig. S6. Nyquist plots for the SC-7 and SC-8 electrode.

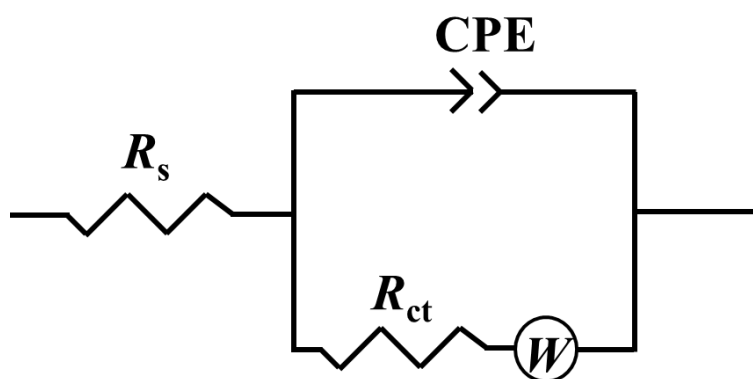


Fig. S7. Simulated equivalent circuit for the as-synthesized Mn-MOFs-based electrodes.

6. Pristine interpenetrated MOFs for endurance tests

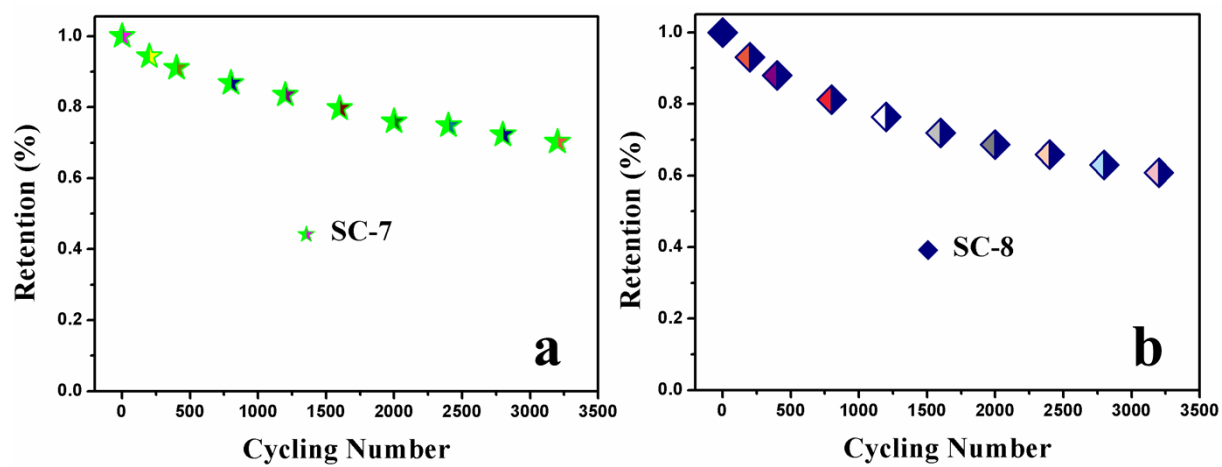


Fig. S8. The capacity retention for SC-7 (a) and SC-8 (b) electrode after 3200 continuous cycles, respectively.

7. Morphology alternation of pristine MOFs electrodes for endurance tests

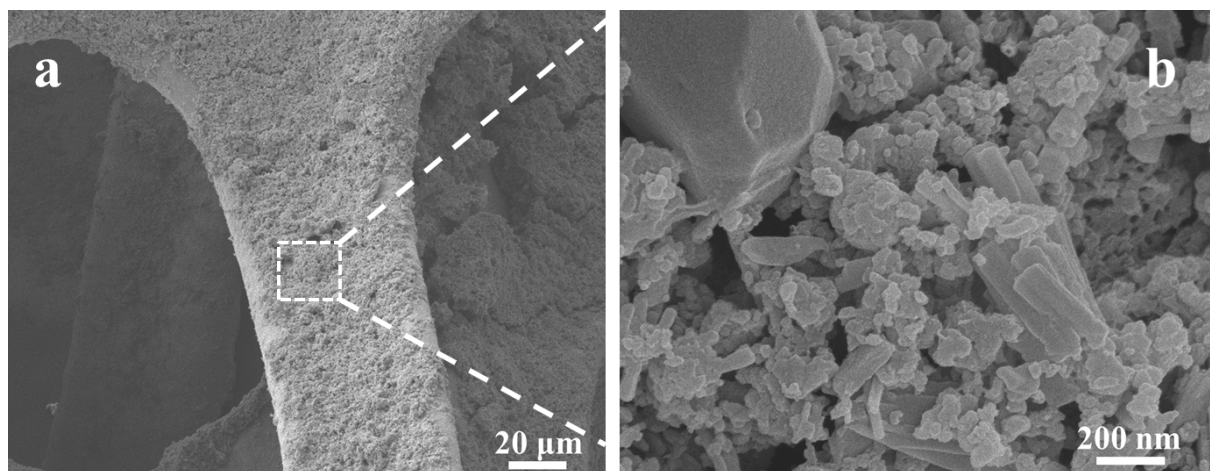


Fig. S9. (a-b) SEM images of SC-7 electrode before 3200 continuous cycles.

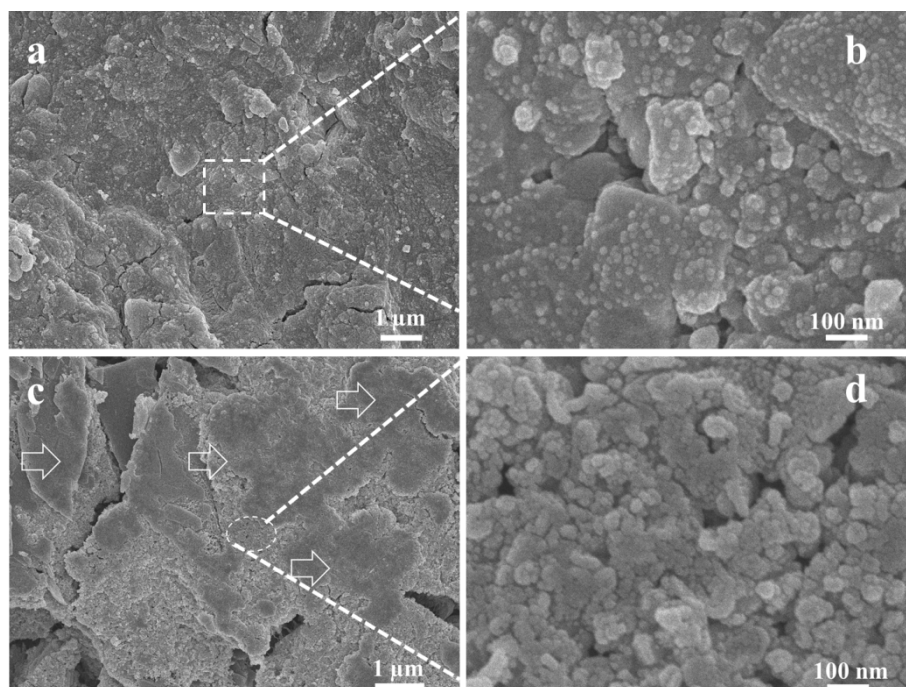


Fig. S10. SEM images of SC-8 electrode before (a-b) and after (c-d) 3200 continuous cycles.

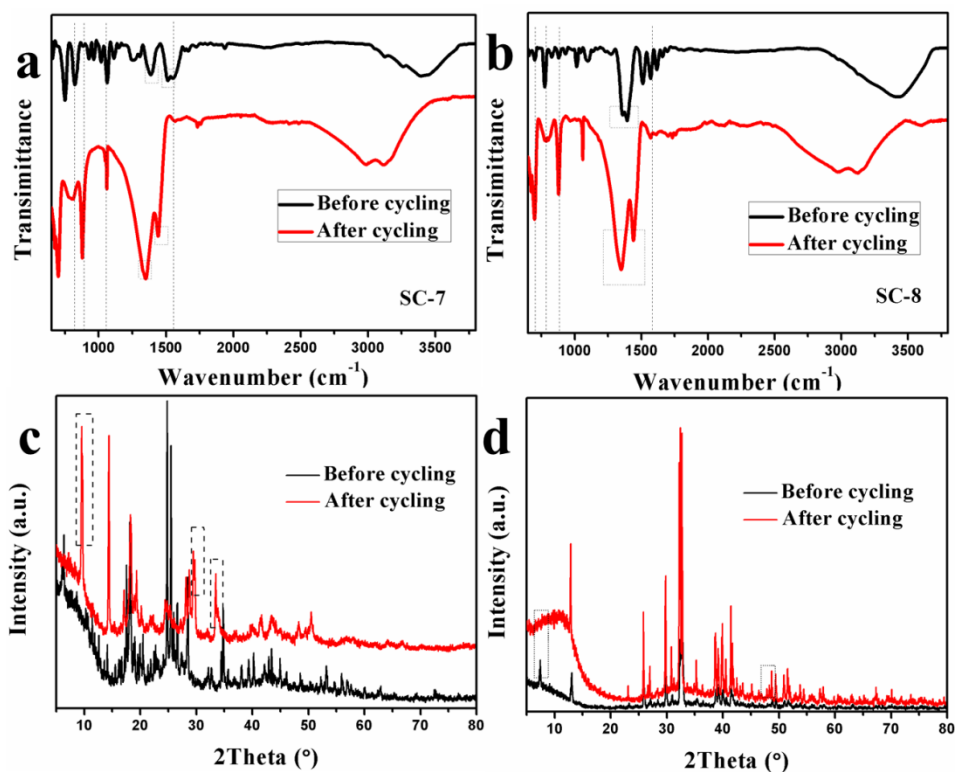


Fig. S11. (a-b) ATR-IR spectra of SC-7 and SC-8 electrode (together with PTFE and acetylene black) before and after 3200 cycles. The dash lines displayed the same peaks remained to indicate the stable frameworks of MOFs and the dash boxes suggested a slight shift for $-\text{COOH}$ group before and after cycling. (c-d) XRD patterns for SC-7 and SC-8 electrode (together with PTFE and acetylene black) before and after 3200 cycles. The dash boxes indicated that some peaks are vanished or shown up after 3200 cycles while the main frameworks were still maintained. These results suggested the structural alternation occurred during the electrochemical process, in keeping with the SEM results.

8. Comparing capacity performances after adding carbon-nanotubes

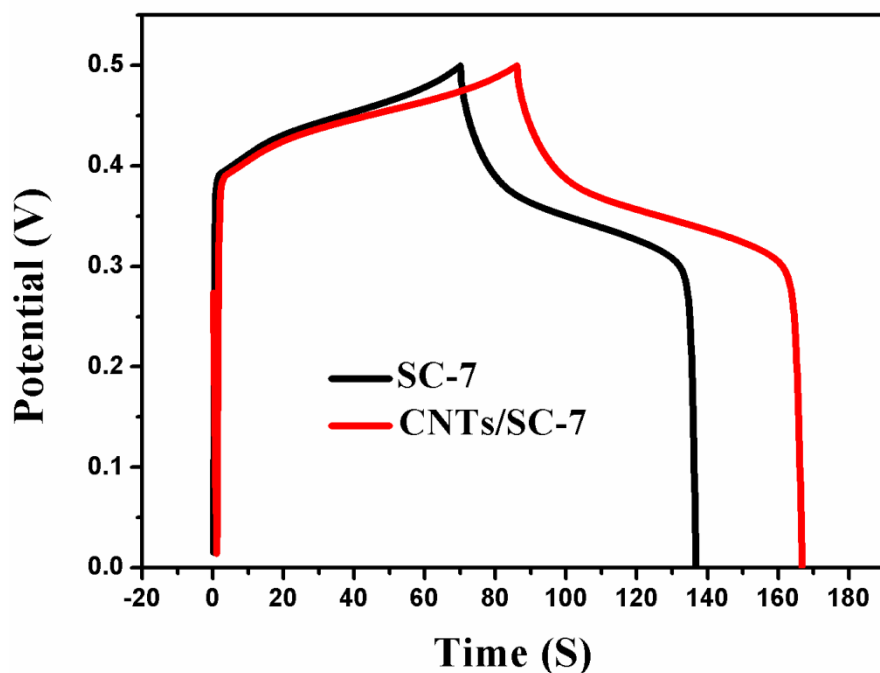


Fig. S12. Compared CD curves of SC-7 and CNTs/SC-7 electrodes at a nominal current density of 10 A g^{-1} .

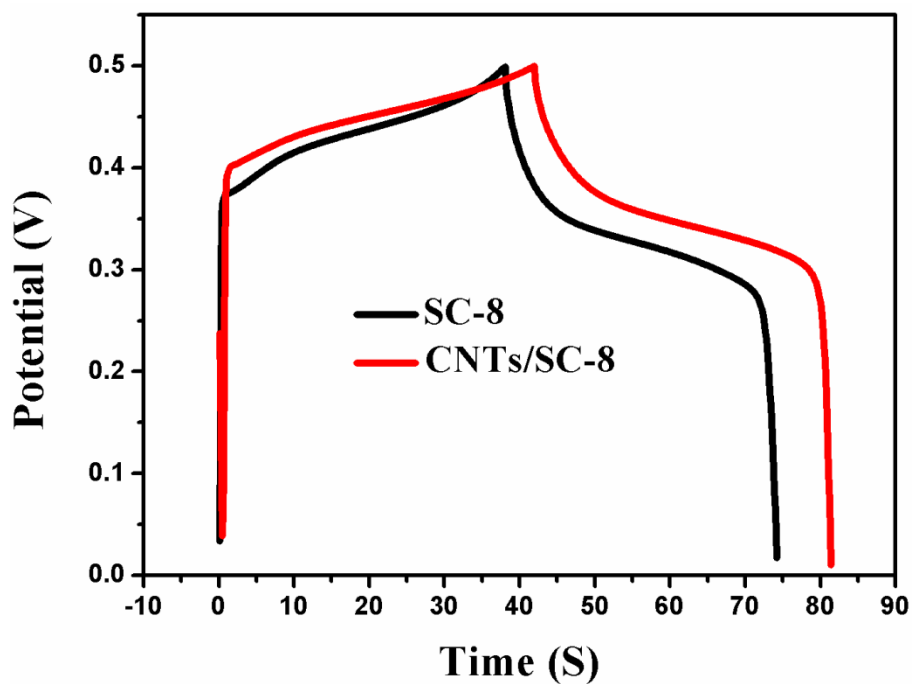


Fig. S13. Compared CD curves of SC-8 and CNTs/SC-8 electrodes at a nominal current density of 10 A g^{-1} .

9. Cycling tests and morphology characterization for CNTs/MOFs.

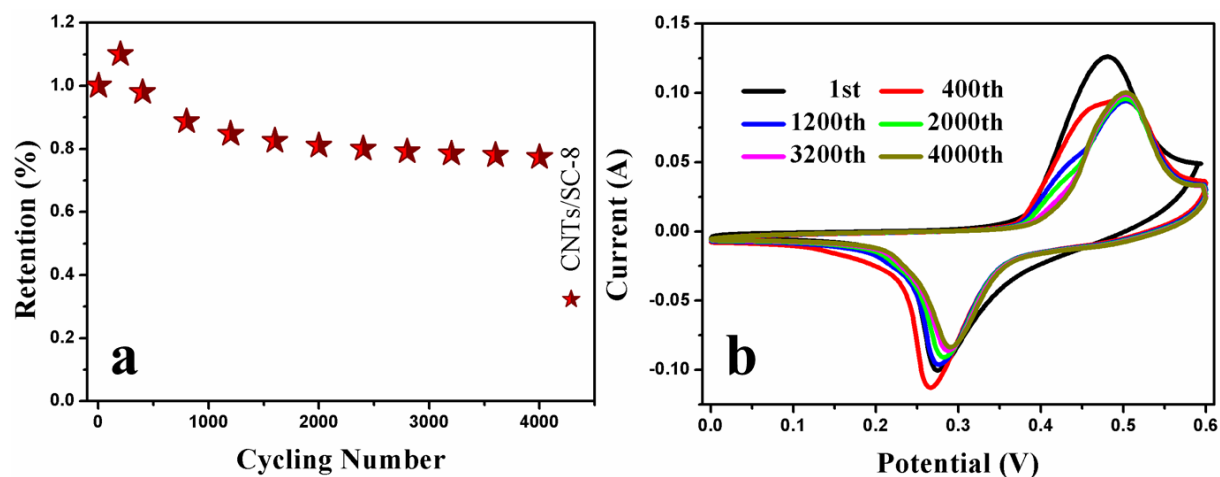


Fig. S14. (a) The various plots of the capacity for CNTs/SC-8 electrode with the increase of cycling numbers. (b) Endurance measurements after 4000 unceasing cycles at a sweep rate of 20 mV s^{-1} .

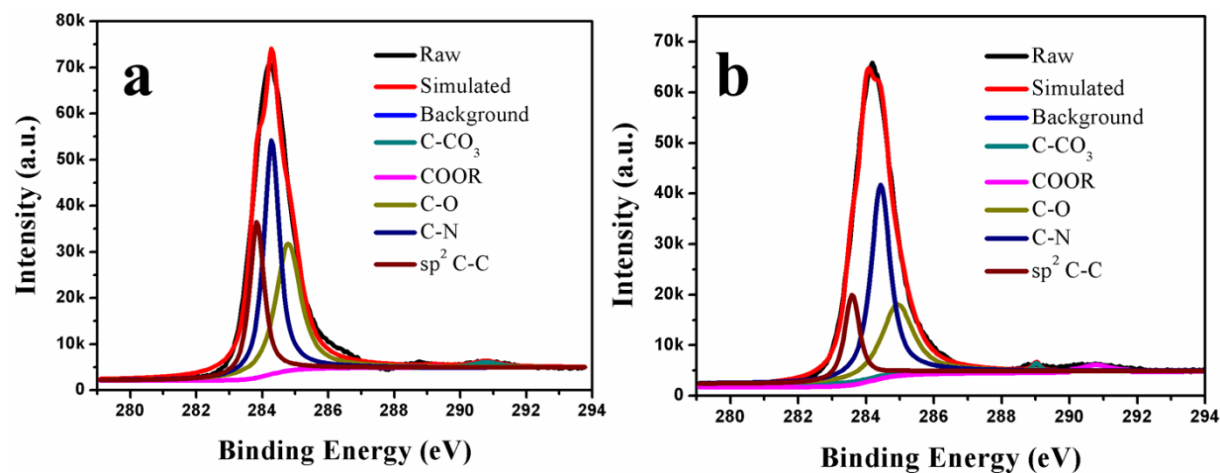


Fig. S15. Deconvoluted C 1s spectra of CNTs/SC-7 (a) and CNTs/SC-8 (b) sample.

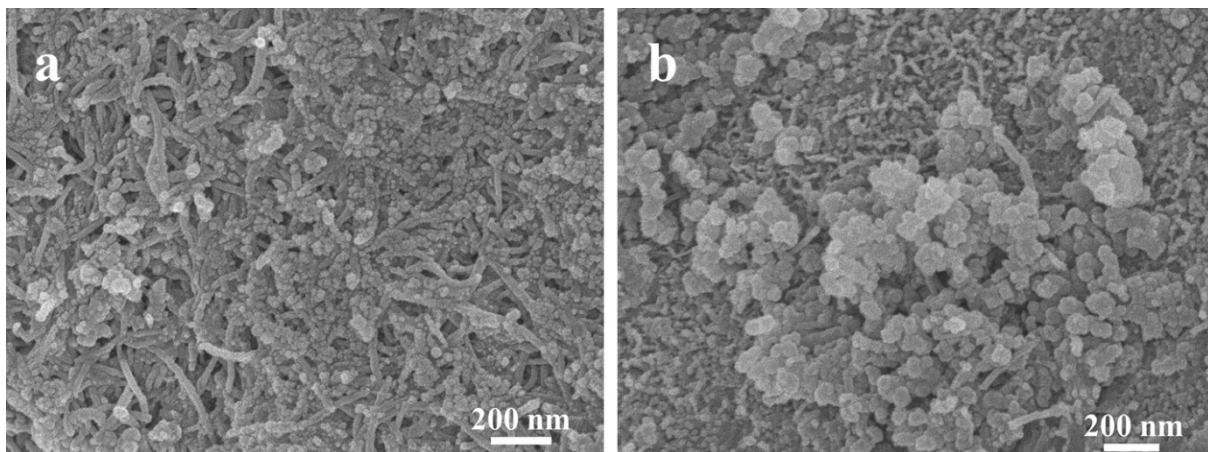


Fig. S16. (a) SEM images of CNTs/SC-8 electrode before cycling. (b) SEM images of CNTs/SC-8 electrode after 4000 continuous cycles.